Electronic Supplementary Information (ESI)

Rapid ionic conductivity of ternary composite electrolytes for superior solid-state batteries with high rate and long cycle life operated at room temperature

Wei Xiong,[ab+] Tao Huang,[a+] Yuqing Feng,[a+] Xue Ye,[a] Xiaoyan Li,[a] Jianneng Liang,[a] Shenghua Ye,[ac] Xiangzhong Ren,[a] Yongliang Li,[a] Qianling Zhang, *[a] Jianhong Liu*[ac]

[a] Graphene Composite Research Center, College of Chemistry and Environmental Engineering, Shenzhen University, 518060, P.R. China

[b] College of Physics and Optoelectronic Engineering, Shenzhen University, Shenzhen, 518060, P.R. China

[c] Shenzhen Eigen-Equation Graphene technology Co. Ltd, Shenzhen, 518060, P.R. China

*Corresponding authors

+Contribute equally to this work

Email address: liujh@szu.edu.cn (J. Liu), zhql@szu.edu.cn (Q. Zhang)

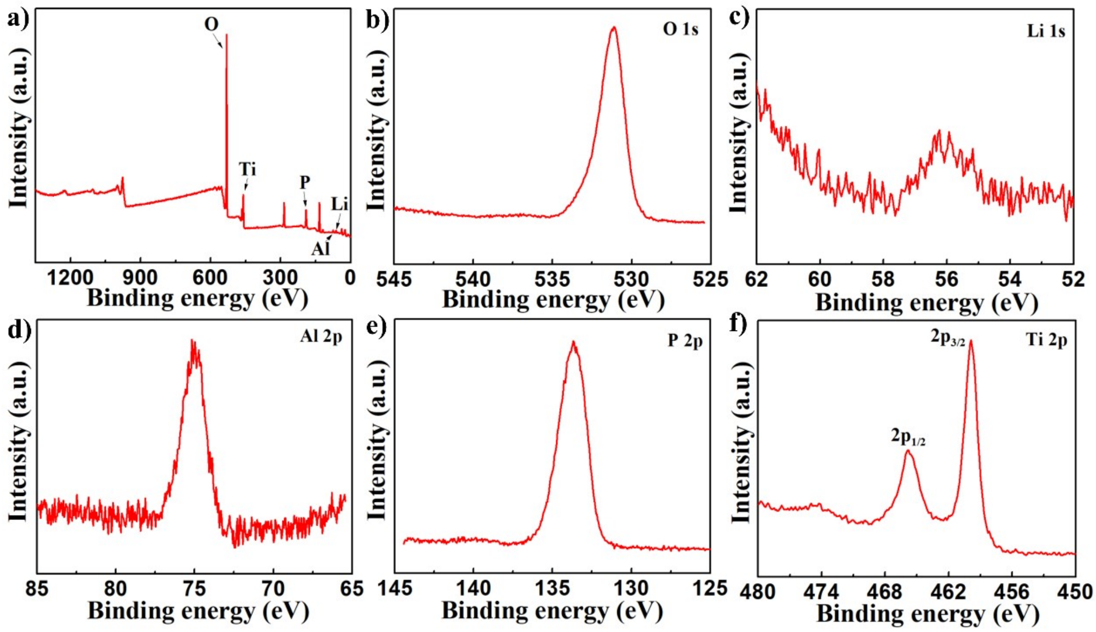

Figure S1. XPS spectra of LATP.

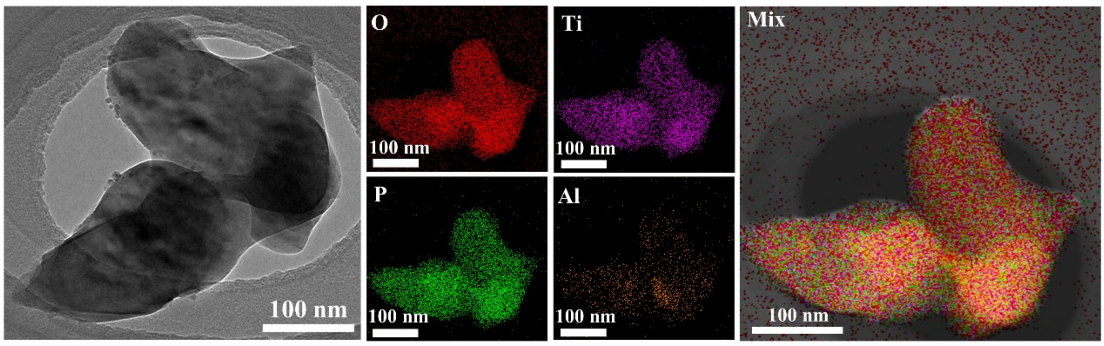

Figure S2. TEM and elemental mapping images of LATP particles.

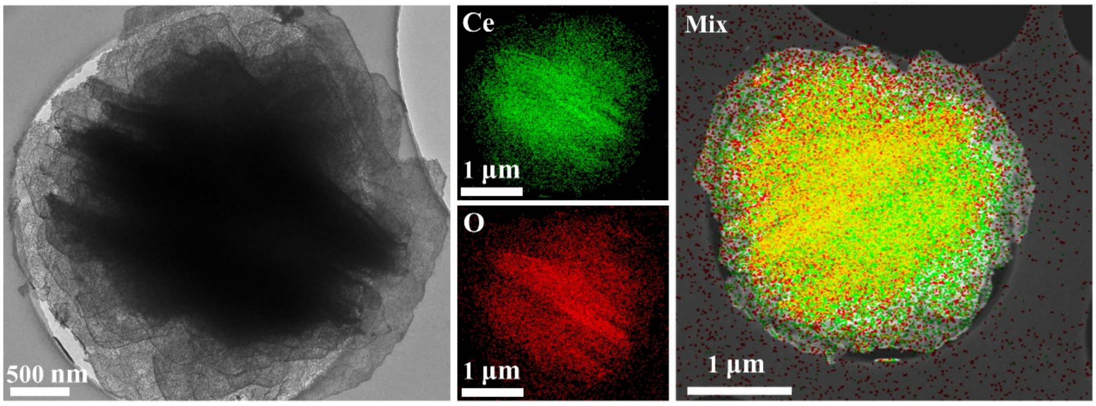

Figure S3. TEM and elemental mapping images of flower-like CeO_2.

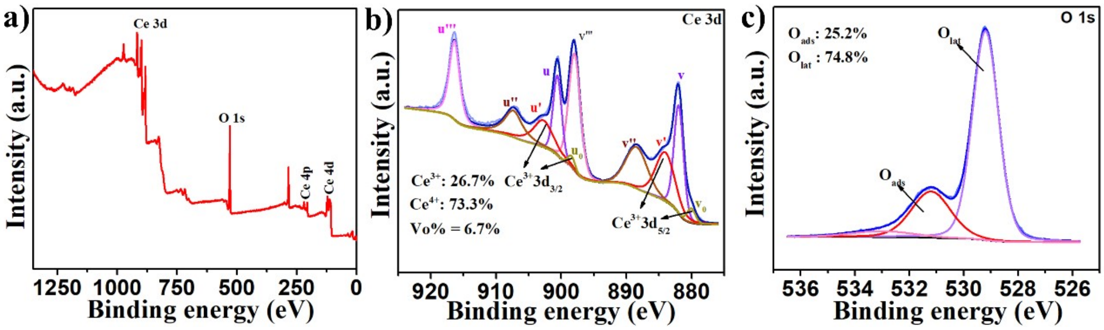

Figure S4. XPS spectra of the flower-like CeO_2 particles with oxygen vacancies (a) survey spectrum, (b) Ce 3d, and (c) O 1s.

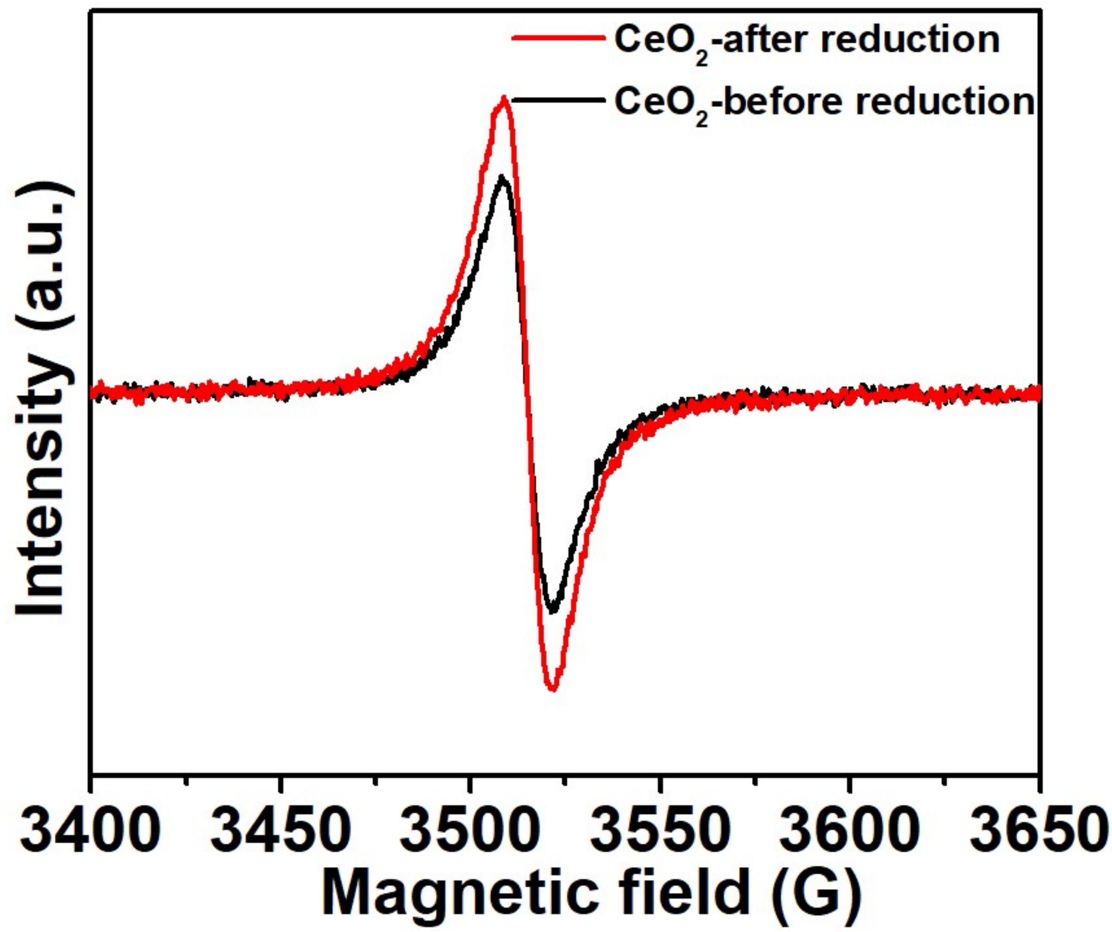

Figure S5. EPR spectra of flower-like CeO_2 particles before and after hydrogen reduction.

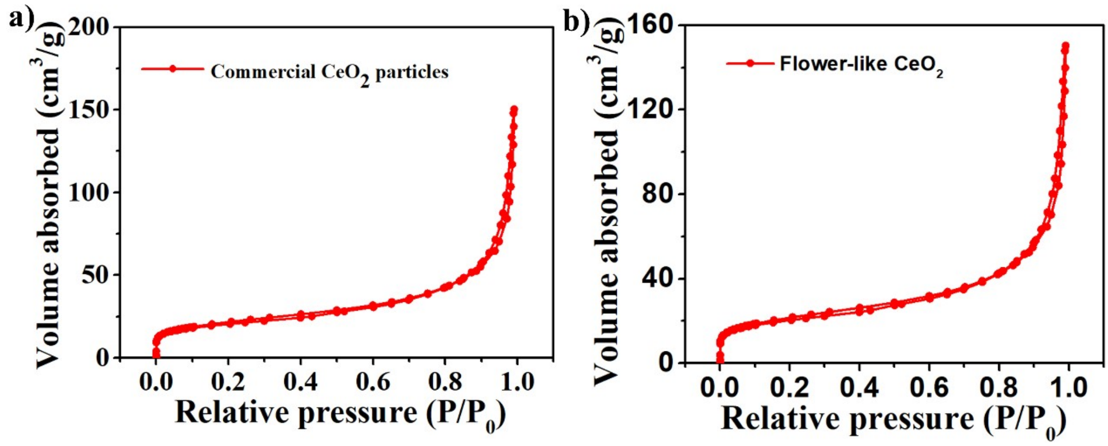

Figure S6. Nitrogen adsorption-desorption isotherms of (a) commercial CeO_2 particles, (b) flower-like CeO_2.

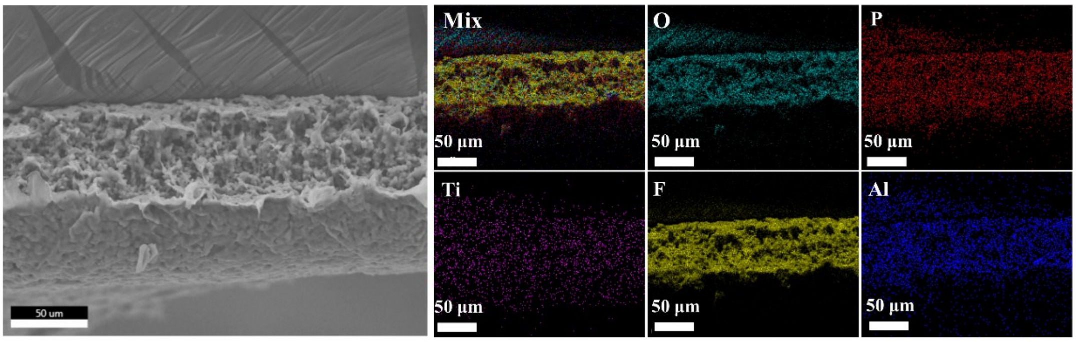

Figure S7. Elemental mapping of the cross-sectional PVDF-HFP/LiTFSI/LATP film.

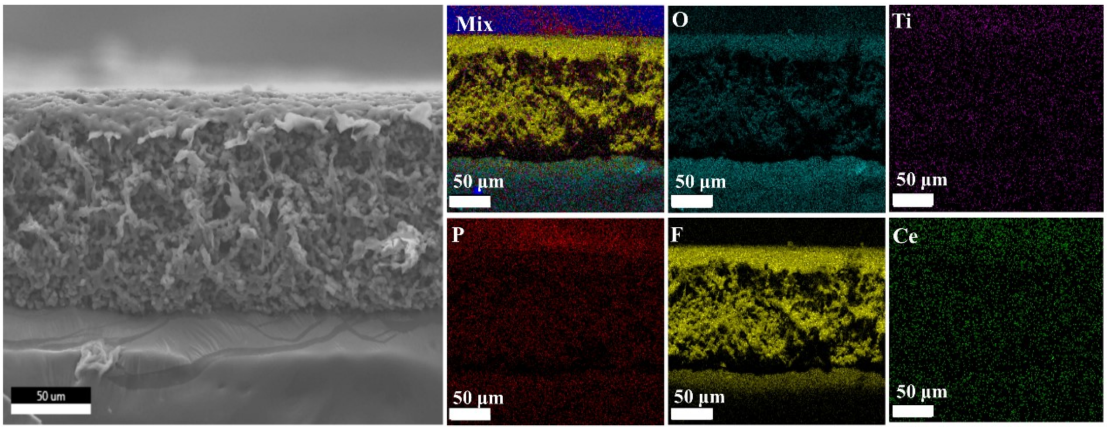

Figure S8. Elemental mapping of the cross-sectional PVDF-HFP/LiTFSI/LATP/CeO_2 film.

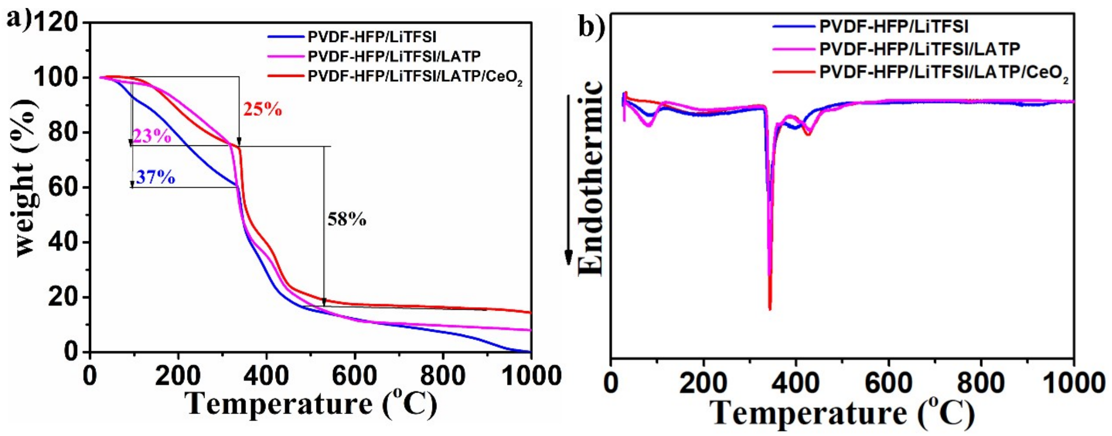

Figure S9. (a) TGA and (b) Differential Thermal Analysis (DTA) curves of PVDF-HFP/LiTFSI, PVDF-HFP/LiTFSI/LATP and PVDF-HFP/LiTFSI/LATP/CeO_2 CSEs.

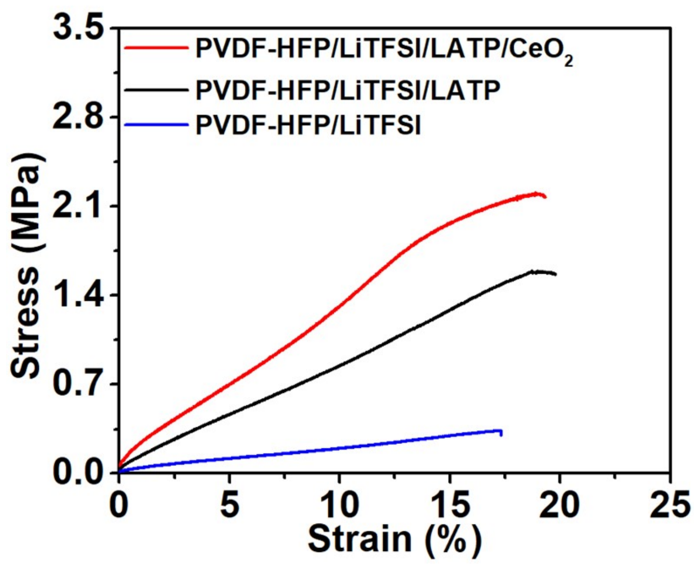

Figure S10. Stress-strain curves of PVDF-HFP/LiTFSI, PVDF-HFP/LiTFSI/LATP, PVDF-HFP/LiTFSI/LATP/CeO_2 films.

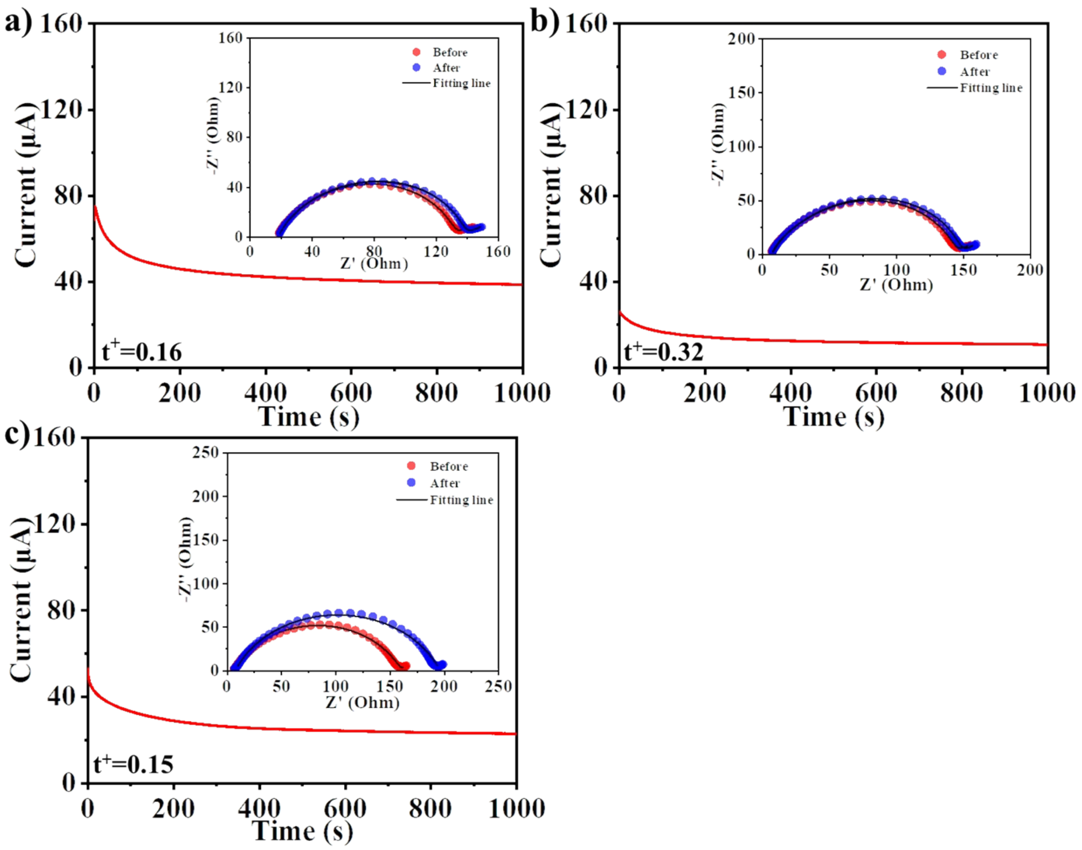

Figure S11. Chronoamperometry curves of (a) PVDF-HFP/LiTFSI/LATP, (b) PVDF-HFP/LiTFSI/CeO_2 and (c) PVDF-HFP/LiTFSI under a potential step of 10 mV at room temperature.

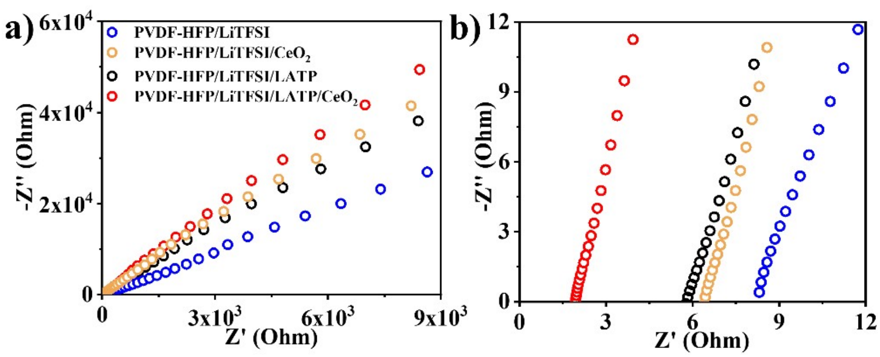

Figure S12. (a) Nyquist plots of SS/CSE/SS cells with the PVDF-HFP/LiTFSI, PVDF-HFP/LiTFSI/CeO_2, PVDF-HFP/LiTFSI/LATP and PVDF-HFP/LiTFSI /LATP/CeO_2 as electrolytes, before electrochemical cycling test. (b) The image of the magnified region with high frequency.

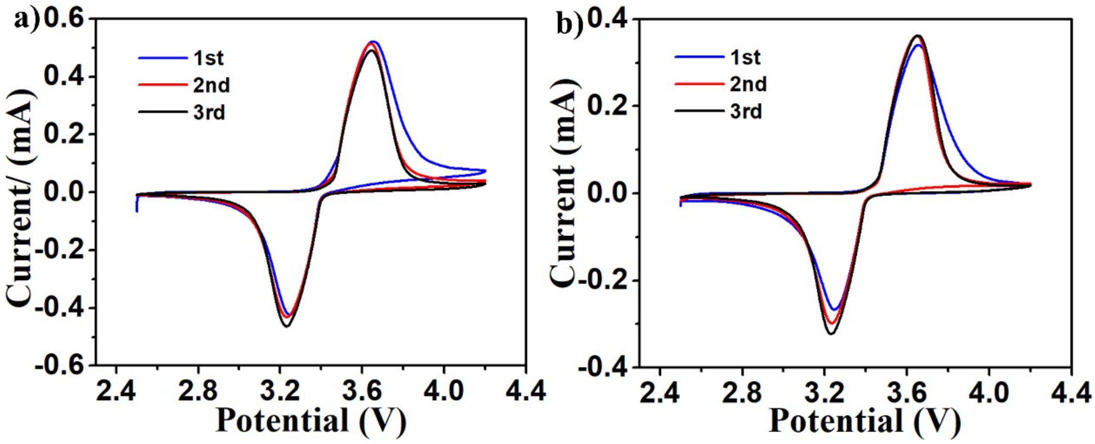

Figure S13. CV curves of LFP cells with (a) PVDF-HFP/LiTFSI/LATP, and (b) PVDF-HFP/LiTFSI/LATP/CeO_2 as the electrolyte.

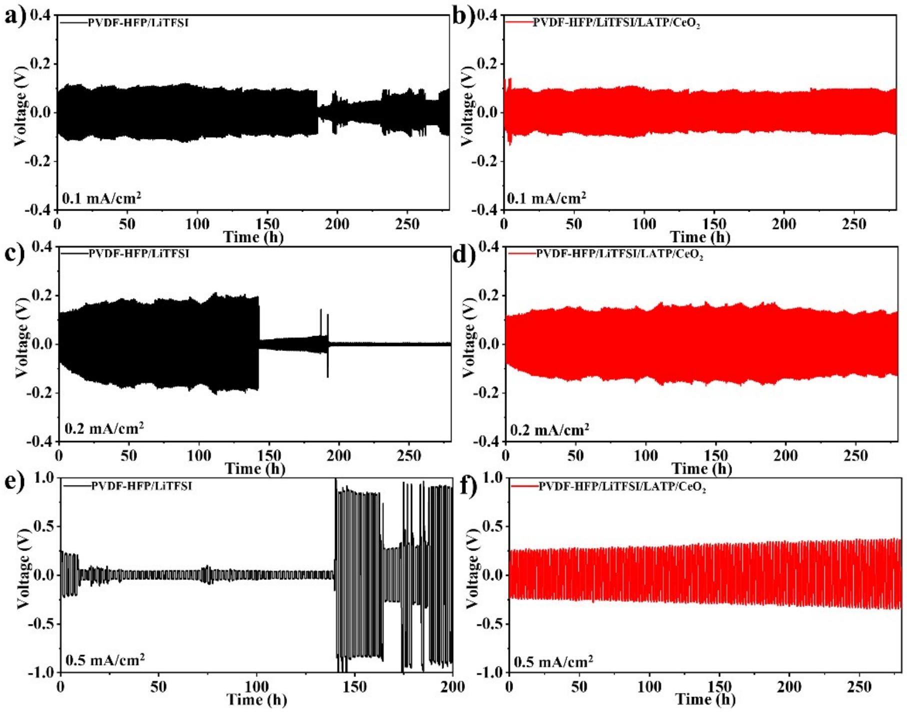

Figure S14. Voltage-time profile of Li/(PVDF-HFP/LiTFSI)/Li and Li/(PVDF-HFP/LiTFSI/LATP/CeO_2)/Li at 0.1, 0.2 and 0.5 mA cm^{-2}.

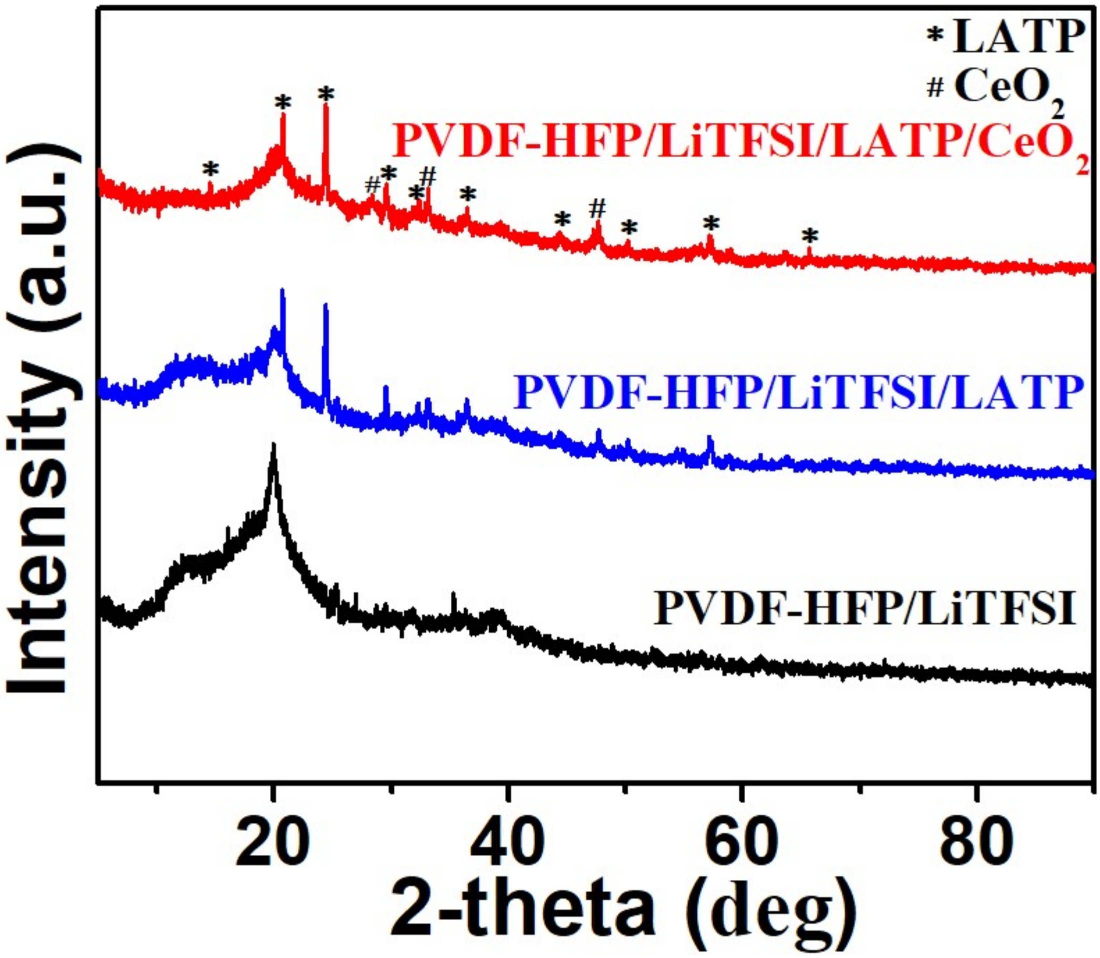

Figure S15. XRD patterns of the PVDF-HFP/LiTFSI, PVDF-HFP/LiTFSI/LATP, PVDF-HFP/LiTFSI/LATP/CeO_2 electrolytes in the LFP cells after electrochemical cycles at 2 C.

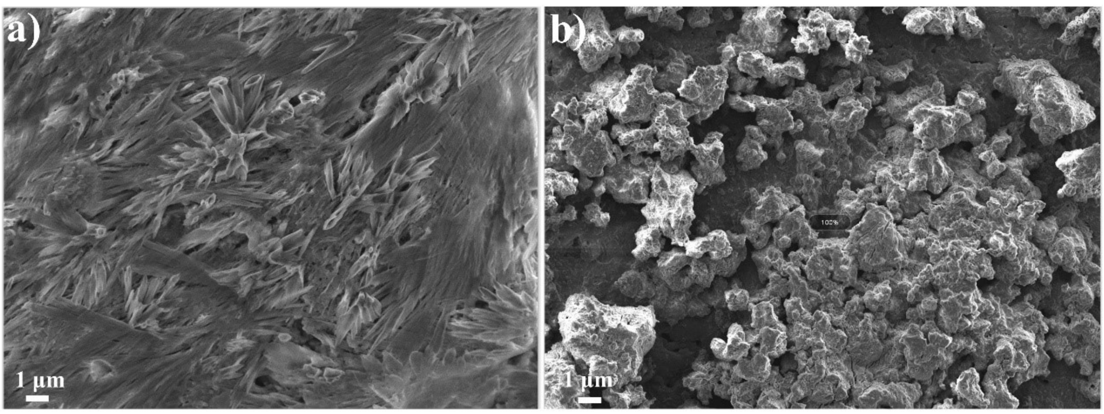

Figure S16. SEM images of the surface morphologies of (a) PVDF-HFP /LiTFSI/LATP and (b) PVDF-HFP/LiTFSI /LATP /CeO_2 CSEs after plating/stripping cycles.

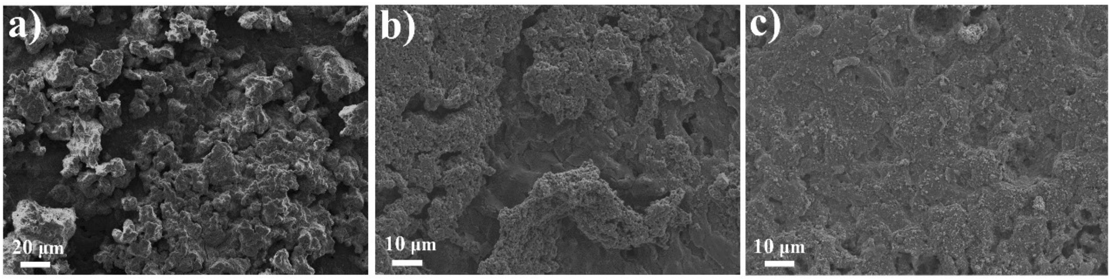

Figure S17. SEM images of surface morphologies of (a) PVDF-HFP/LiTFSI, (b) PVDF-HFP/LATP/LiTFSI, and (c) PVDF-HFP/LiTFSI/LATP/CeO_2 films contacted with Li metal after 1000 cycles at 2 C.

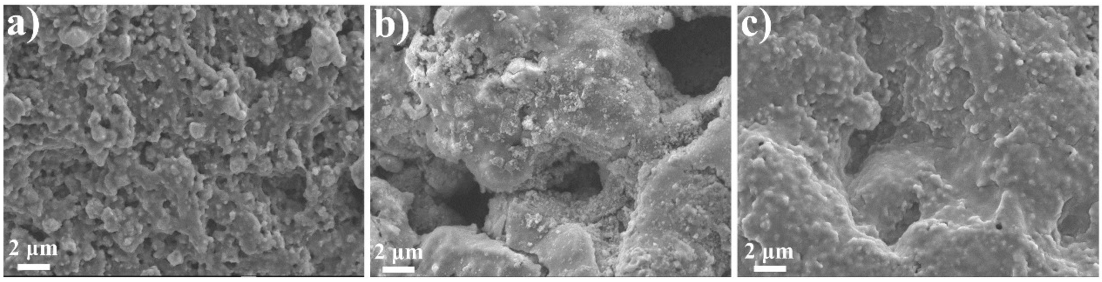

Figure S18. SEM images of the surface morphologies of (a) PVDF-HFP/LiTFSI, (b) PVDF-HFP/LATP/LiTFSI, and (c) PVDF-HFP/LiTFSI/LATP/CeO_2 films contacted with LFP cathode after 1000 cycles at 2 C.

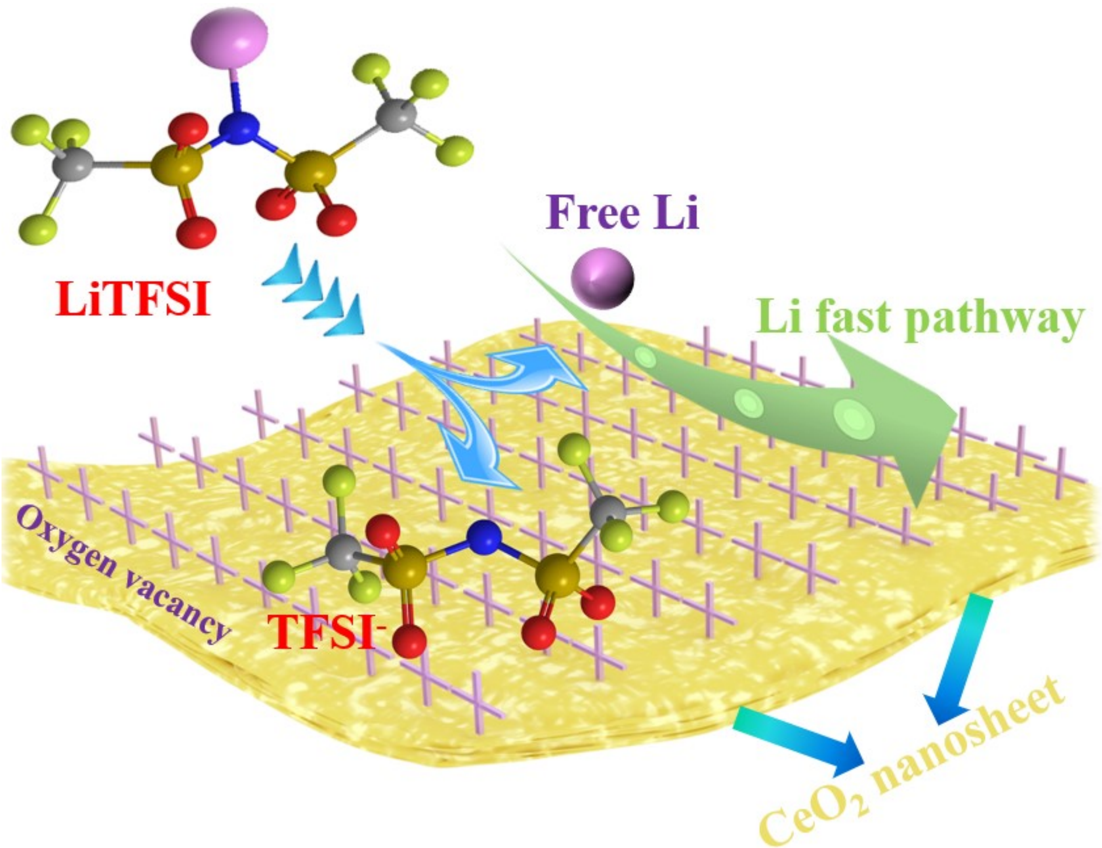

Figure S19. Schematic illustration of the dissociation process of LiTFSI induced by CeO_2 with oxygen vacancies.

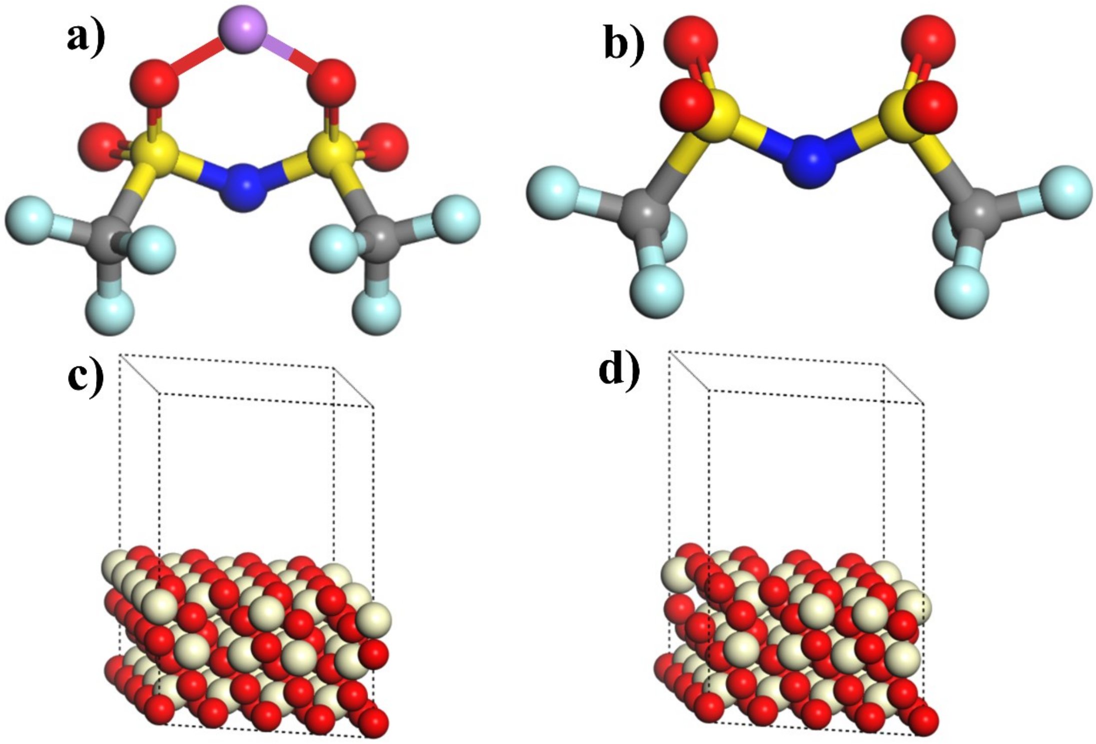

Figure S20. The molecular structures with the lowest energy conformation of a) LiTFSI and b) $TFSI^-$ anion.

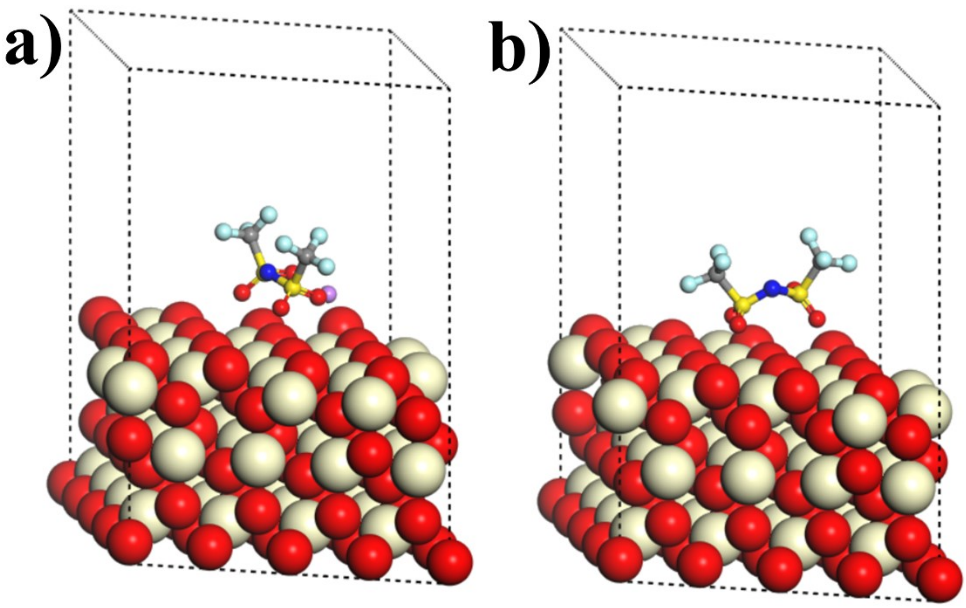

Figure S21. The most stable crystallographic structures of (a,c) LiTFSI, and (b,d) TFSI- anion adsorbed on the CeO_2 (111) surface atomic structure. O in red, Ce in light yellow, C in gray, F in light blue, S in yellow, N in blue, Li in purple.

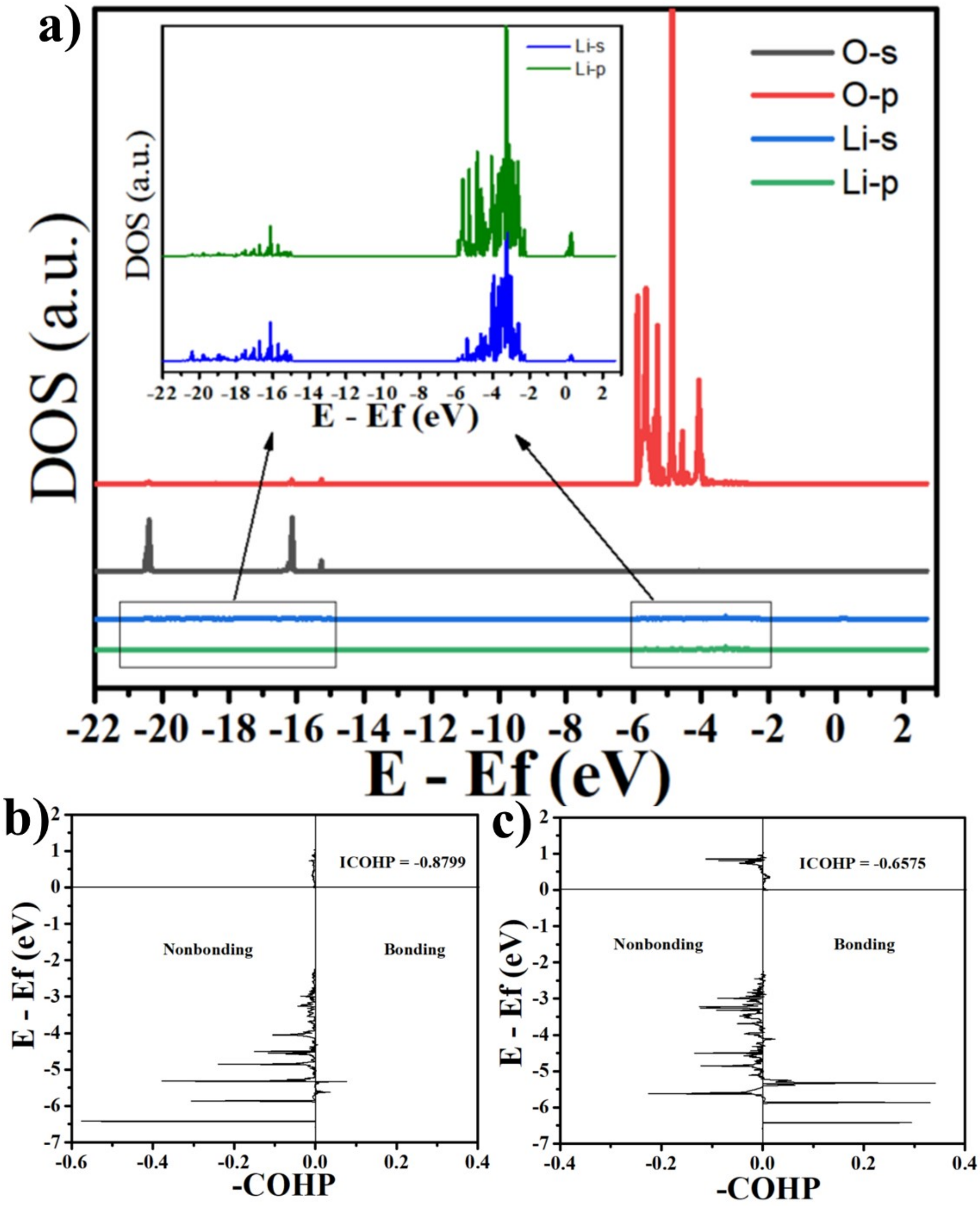

Figure S22. (a) PDOS, and (b,c) COHP images of the interaction between LiTFSI and CeO_2 (111) surface with one oxygen vacancy.

Table S1. Peak positions and areas for core level of Ce 3d in CeO_2 nanosheets

	peaks	u'''	u''	u	v'''	v''	v
Ce^{4+}3d	BE(eV)	916.38	907.33	900.59	897.96	888.43	881.99
	area	70181.77	8920	54064	04748.9	67884.88	76596.84
Ce^{3+}3d	peaks	u'	v'	u_0	v_0		
	BE(eV)	902.74	884.06	898.42	880.08		
	area	49558.55	74337.83	6132.386	9198.579		
$[Ce^{3+}]$ = 26.7%, $[Ce^{4+}]$ = 73.3%, [Vo]= 6.7%							

Table S2. Peak positions and areas for core level of O 1s in CeO_2 nanosheets.

	peaks	O_{ads}	O_{lat}
O 1S	BE(eV)	531.2	529.2
	area	27947.98	83029.78
$[O_{ads}]$=25.2%, $[O_{lat}]$=74.8%			

Table S3. Comparison of electrochemical performance between our work and reported state-of-the-art CSEs.

CSEs composition	Ionic conductivity /Temperature	Electrochemical window (V)	Li^+ transfer number	Specific capacity of LFP cells/Temperature	Reference
PVDF-HFP/LATP/CeO_2	**1.66 × 10^{-3} S cm^{-1} 25 °C**	**5.1**	**0.35**	**166.6 mAh g^{-1} at 0.1 C, 83.1 mAh g^{-1} at 2 C after 1000 cycles 25 °C**	**This work**
Ca–CeO_2/PEO	1.3 × 10^{-4} S cm^{-1} 60 °C	4.5	0.453	93 mAh g-1 after 200 cycles at 1 C 60 °C	Adv. Energy Mater.[1]
CeO_2/PEO	1.1 × 10^{-3} S cm^{-1} 60 °C	5.1	0.47	160 mAh g^{-1} at 0.1 C 60 °C	Nano Energy[2]
CeO_2/PEO/liquid electrolyte	9.09 × 10^{-5} S cm^{-1} 30 °C	4.89	0.4	155.3mAh g^{-1} after 130 cycles at 1 C and 30 °C	J. Membr. Sci.[3]
PEG-MDI/LiDMPA	1 × 10^{-4} S cm^{-1} 25 °C	5	0.72	159 mAh/g 50th 99.1% at 0.2 C 80 °C	J. Mater. Chem. A[4]
LLTO/PEO/FEC	1.13 × 10^{-4} S cm^{-1} 25 °C	5.2	0.35	86 mAh·g^{-1} at 0.5 C 35 °C	Chem. Eng. J.[5]
PEO/$CsClO_4$	1.9 × 10^{-4} S cm^{-1} 60 °C	4.35	NA	120 mAh·g^{-1} at 0.5 C 60 °C	Energy Storage Mater.[6]
LLZTO/PEO	2.3 × 10^{-5} S cm^{-1} 30 °C	5.03	0.47	100 mAh·g^{-1} at 0.1 C 30 °C	Adv. Energy Mater.[7]
SiO_2 areogel/PEO	6 × 10^{-4} S cm^{-1} 60 °C	5	NA	110 mAh·g^{-1} at 0.5 C 25 °C	Adv. Mater.[8]
PEO/ionic liquid	5.01 × 10^{-4} S cm^{-1} 60 °C	5.26	0.34	160.3 mAh g^{-1} at 0.2 C 60 °C	Energy Storage Mater.[9]
PVDF/PEO	NA	4	NA	97.8 mAh g-1 at 1 C	Chem. Eng.

				after 600 cycles 70 °C	J.[10]
PEO/BN	1.45 × 10^{-4} S cm^{-1} 80 ºC	5.16	0.33	143.3 mAh·g^{-1} at 0.1 C 60 °C	J. Mater. Chem. A[11]
PEO/HPMA	1.13 × 10^{-4} S cm^{-1} 35 ºC	5.1	0.22	80.4 mAh g^{-1} at 1 C after 1255 cycles 35 °C	J. Mater. Chem. A[12]
PVDF-HFP/LLATO/Li_3PO_4	5.1 × 10^{-4} S cm^{-1} 25 ºC	5	0.45	76 mAh g^{-1} at 2 C 25 °C	J. Mater. Chem. A[13]
LLZAO/PEO	2.5 × 10^{-4} S cm^{-1} 25 ºC	5.58	0.53	84.1 mAh g^{-1} at 1 C 25 °C	Chem. Eng. J.[14]
PEO/LAGP	1.67 × 10^{-4} S cm^{-1} 25 ºC	NA	0.56	148.7 mAh g^{-1} at 0.2 C 25 °C	Nano Energy[15]
Cellulose/LAGP	1.1 × 10^{-4} S cm^{-1} 60 ºC	4.96	NA	148 mAh g^{-1} at 0.1 C 60 °C	Nano Lett.[16]
PVDF/LLZTO	8.8 × 10^{-5} S cm^{-1} 25 ºC	4.25	NA	154.9 mAh g^{-1} at 0.1 C 55 °C	Chem. Eng. J.[17]
PEO/aramid	8.8 × 10^{-5} S cm^{-1} 25 ºC	4.2	NA	152 mAh g^{-1} at 0.1 C 50 °C	Nano Energy[18]
PEO/$LiZr_2(PO_4)_3$	1.2 × 10^{-4} S cm^{-1} 30 ºC	4.8	0.36	155 mAh g^{-1} at 100 uA cm^{-2} 30 ºC	J. Am. Chem. Soc.[19]
PEO/PDA/LLZTO	1.1 × 10^{-4} S cm^{-1} 30 ºC	4.8	NA	129.5 mAh g^{-1} at 0.2 C 50 °C	J. Mater. Chem. A[20]
PEO/SiO_2/Li_2SO_4	1.3 × 10^{-4} S cm^{-1} 60 ºC	5	0.45	80 mAh g^{-1} at 0.5 C 60 °C	Small[21]
PEO/vermiculite	7.9 × 10^{-7} S cm^{-1} 25 ºC	5.35	0.246	159.9 mAh g^{-1} at 0.1 C 60 °C	Adv. Energy Mater.[22]

Reference

1. H. Chen, D. Adekoya, L. Hencz, J. Ma, S. Chen, C. Yan, H. J. Zhao, G. L. Cui and S. Q. Zhang, *Adv Energy Mater.*, 2020, **10,** 2000049.

2. X. Ao, X. Wang, J. Tan, S. Zhang, C. Su, L. Dong, M. Tang, Z. Wang, B. Tian and H. Wang, *Nano Energy*, 2021, **79**, 105475.
3. P. Lun, P. Liu, H. Lin, Z. Dai, Z. Zhang and D. Chen, *J. Memb. Sci.*, 2019, **580**, 92-100.
4. Z. K. Zhao, Y. M. Zhang, S. J. Li, S. H. Wang, Y. L. Li, H. W. Mi, L. N. Sun, X. Z. Ren and P. X. Zhang, *J. Mater. Chem. A*, 2019, **7**, 25818-25823.
5. H. Li, W. Liu, X. Yang, J. Xiao, Y. Li, L. Sun, X. Ren, P. Zhang and H. Mi, *Chem. Eng. J.*, 2021, **408**, 127254.
6. X. Yang, Q. Sun, C. Zhao, X. Gao, K. Adair, Y. Zhao, J. Luo, X. Lin, J. Liang, H. Huang, L. Zhang, S. Lu, R. Li and X. Sun, *Energy Storage Mater.*, 2019, **22**, 194-199.
7. H. Huo, Y. Chen, J. Luo, X. Yang, X. Guo and X. Sun, *Adv. Energy Mater.*, 2019, **9**, 1804004.
8. D. Lin, P. Y. Yuen, Y. Liu, W. Liu, N. Liu, R. H. Dauskardt and Y. Cui, *Adv. Mater.*, 2018, **30**, 1802661.
9. J. Tan, X. Ao, A. Dai, Y. Yuan, H. Zhuo, H. Lu, L. Zhuang, Y. Ke, C. Su, X. Peng, B. Tian and J. Lu, *Energy Storage Mater.*, 2020, **33**, 173-180.
10. L. Gao, J. Li, J. Ju, L. Wang, J. Yan, B. Cheng, W. Kang, N. Deng and Y. Li, *Chem. Eng. J.*, 2020, **389**, 124478.
11. Y. Li, L. Zhang, Z. Sun, G. Gao, S. Lu, M. Zhu, Y. Zhang, Z. Jia, C. Xiao, H. Bu, K. Xi and S. Ding, *J. Mater. Chem. A*, 2020, **8**, 9579-9589.
12. G. Wang, X. Zhu, A. Rashid, Z. Hu, P. Sun, Q. Zhang and L. Zhang, *J. Mater. Chem. A*, 2020, **8**, 13351-13363.
13. H. Yang, J. Bright, B. Chen, P. Zheng, X. Gao, B. Liu, S. Kasani, X. Zhang and N. Wu, *J. Mater. Chem. A*, 2020, **8**, 7261-7272.
14. D. Cai, D. Wang, Y. Chen, S. Zhang, X. Wang, X. Xia and J. Tu, *Chem. Eng. J.*, 2020, **394**, 124993.
15. X. Wang, H. Zhai, B. Qie, Q. Cheng, A. Li, J. Borovilas, B. Xu, C. Shi, T. Jin, X. Liao, Y. Li, X. He, S. Du, Y. Fu, M. Dontigny, K. Zaghib and Y. Yang, *Nano Energy*, 2019, **60**, 205-212.
16. C. Wang, D. Huang, S. Li, J. Yu, M. Zhu, N. Liu and Z. Lu, *Nano Lett.*, 2020, **20**, 7397-7404.
17. J. Lu, Y. Liu, P. Yao, Z. Ding, Q. Tang, J. Wu, Z. Ye, K. Huang and X. Liu, *Chem. Eng. J.*, 2019, **367**, 230-238.
18. L. Liu, J. Lyu, J. Mo, H. Yan, L. Xu, P. Peng, J. Li, B. Jiang, L. Chu and M. Li, *Nano Energy*, 2020, **69**, 104398.
19. N. Wu, P.-H. Chien, Y. Li, A. Dolocan, H. Xu, B. Xu, N. S. Grundish, H. Jin, Y.-Y. Hu and J. B. Goodenough, *J. Am. Chem. Soc.*, 2020, **142**, 2497-2505.
20. Z. Huang, W. Pang, P. Liang, Z. Jin, N. Grundish, Y. Li and C.-A. Wang, *J. Mater. Chem. A*, 2019, **7**, 16425-16436.
21. J. Yu, C. Wang, S. Li, N. Liu, J. Zhu and Z. Lu, *Small*, 2019, **15**, 1902729.
22. W. Tang, S. Tang, C. Zhang, Q. Ma, Q. Xiang, Y.-W. Yang and J. Luo, *Adv. Energy Mater.*, 2018, **8**, 1800866.